RSC Advances

PAPER

View Article Online
View Journal | View Issue

Cite this: *RSC Adv.*, 2025, **15**, 34473

Bioinspired reconfigurable cloverleaf DNA origami as a versatile platform for visual molecular detection

Si Sun,[ab] Xi Shu,[a] Xin Chen,[a] Fang Wang,[a] Xiao-Li Qiang,[a] Qian-Ru Xiao *[a] and Xiao-Long Shi *[a]

Received 16th August 2025
Accepted 16th September 2025

DOI: 10.1039/d5ra06047h

rsc.li/rsc-advances

DNA origami technology has revolutionized nanofabrication by enabling the evolution from static nanostructures to programmable dynamic systems. Herein, we present a bioinspired cloverleaf DNA origami system enabling structural reconfiguration, reversible molecular detection, and programmable higher-order assembly. Two basic cloverleaf related DNA origami structures were designed: a flexible four-leaf structure (Leaf4) and a stable four-leaf clover (Lucky4) stabilized by central linker staples, as confirmed by atomic force microscopy (AFM) and simulations (tacoxDNA, CanDo). Leaf4 transitions to a closed doughnut topology *via* apex strand replacement, mimicking water lily closure dynamics. Lucky4 serves as a sensing platform: its blades are functionalized with split capture strands, enabling target sequence binding visualized by AFM and subsequent toehold-mediated release. Extending this strategy, two Lucky4 units assemble into sandwich structures upon target addition, exhibiting double the height of single units. This reconfigurable system integrates biomimetic nanomechanics with visual molecular detection and modular nanostructure assembly.

Introduction

DNA origami technology, as a groundbreaking advancement in nanofabrication, has achieved a transformative leap from static structural assembly to intelligent dynamic systems.[1–4] This technology employs the principle of DNA base-pair complementarity, utilizing the self-assembly of scaffold DNA with staple strands to precisely construct complex 2D/3D nanostructures. With the maturation of computer-aided design tools (*e.g.*, caDNAno), various configurations including triangles and tetrahedral structures can now be efficiently fabricated, demonstrating unique advantages in biosensing and drug delivery applications.[5–7]

Researchers have engineered DNA origami architectures with diverse geometries tailored to specific applications. Seeman *et al.* engineered a cross-shaped DNA origami structure featuring bidirectional helical axes.[8] This design overcomes limitations of unidirectional cohesive-end associations in conventional approaches, enabling programmable 2D array assembly through orthogonal spatial arrangements of vacancy configurations. Chen *et al.* engineered a hexagonal DNA origami structure that can be programmably reconfigured into hexagonal or linear conformations with open/folded patterns.[9] This flexible architecture exhibits robust switchability, enabling dynamic pattern recognition capabilities. They also constructed a predetermined-shape DNA nanostructure *via* combining a rectangular DNA origami frame with DNA SSTs, which used fewer oligonucleotides and circumvented kinetic traps.[10] Qian *et al.* introduced a 'fractal assembly' method that constructs programmable DNA origami arrays through recursive application of local assembly rules, achieving patterns such as the Mona Lisa and a rooster.[11] Moreover, they extended the application of the tile displacement mechanism, and realized the modular reconfiguration of a sword-shaped DNA origami assembly to a snake-shaped assembly.[12,13] Kostiainen *et al.* designed a pliers-like DNA origami which could switch between a cross shape and an "X" shape upon the stimulation of pH change.[14] More interestingly, Kim *et al.* built a DNA wireframe paper and demonstrated a systematic and programmable approach to fold it into various configurations in response to various environmental stimuli.[15] Petersen *et al.* designed a rotationally symmetric triangular origami with maximum continuous surface area, achieving a 20-unit rhombic triacontahedron through edge-directed programming.[16]

In Paul Rothemund's DNA origami designs, hairpin motifs serve as pixels affixed to the scaffold *via* staple strands, forming two-dimensional patterns such as letters and snowflakes.[17] Other DNA modifications, such as biotin and streptavidin could serve as alternative labelling strategies. Wang *et al.* applied

[a]*Institute of Computing Science and Technology, Guangzhou University, Guangzhou 510006, People's Republic of China*

[b]*School of Computer Science of Information Technology, Qiannan Normal University for Nationalities, Duyun 558000, People's Republic of China. E-mail: qianrushaw@gzhu.edu.cn; xlshi@gzhu.edu.cn*

biotin-streptavidin at specific sites of B1 and B2 to differentiate two types of DNA origami building block pieces under AFM.[18]

More significantly, DNA origami technology provides a transformative platform for detection of biomolecules. Song *et al.* developed the first logic-gated sensing platform based on DNA origami for miRNA profiling *via* atomic force microscopy.[19] Andersen *et al.* developed an optical nanobiosensor based on DNA origami technology, which enables rapid detection of target DNA sequences by constructing a multi-fluorophore FRET (Förster resonance energy transfer) signal system through geometrically precise alignment of donor–acceptor fluorescent arrays.[20] Yang *et al.* engineered a rectangular DNA origami scaffold onto which multiple fluorescence-labeled DNA hairpin probes were anchored, enabling catalytic hairpin assembly (CHA)-mediated detection of miRNA-21.[21] Moreover, Lu *et al.* functionalized the DNA origami periphery with cancer-targeting aptamers and precisely patterned two entropy-driven reaction (EDR) circuit substrate modules in an alternating configuration on its surface, leveraging confinement-enhanced kinetics for ultrasensitive miRNA detection.[22]

Inspired by the natural morphology of four-leaf clovers and the circadian rhythms of water lilies (nyctinasty), this study developed a multifunctional platform integrating structural reconfiguration, molecular detection, and hierarchical assembly. By implementing a central junction stabilization design (Lucky4) and a dynamic vertex strand-displacement strategy (Leaf4), we achieved synergistic integration of biomimetic conformational switching and visual nucleic acid detection. Furthermore, through modification of capture strands, programmable molecular recognition and nanoscale "sandwich-type" assembly were accomplished. This work establishes a new paradigm for next-generation dynamic DNA nanodevices, with its unique topological transformation capability and visual signal readout characteristics demonstrating broad application prospects in biosensing and intelligent theragnostic.

Materials and methods

Design of the cloverleaf DNA origami

The cloverleaf DNA origami based on M13mp18 scaffold was designed on a square lattice using caDNAno, and its three-dimensional shape was further evaluated using the CanDo (Computer-aided engineering for DNA origami) software. The main structure consists of four blades (leaves), with their ends connected by several central linker staples. The apex of each blade is closed by a single 32-nucleotide (nt) staple strand. The sequences of M13 scaffold, the staple strands and the central linkers are provided in Table S1.

Preparation of Leaf4 structure. The M13 scaffold and the staple strands excluding the central linker staples were mixed at a 1 : 5 ratio and annealed according to the previous reported experiment.[23] Briefly, the scaffold and staple were first mixed in 1× Tris-acetate-EDTA (TAE) buffer (containing 12.5 nM $MgCl_2$). The mixtures were heated to 95 °C and held for 2 min, then they were annealed at a rate of 6 s per 0.1 °C for 90 min. The annealing process was performed in a thermocycler.

Preparation of Lucky4 structure. The M13 scaffold and the staple strands including the central linker staples were mixed at a 1 : 5 ratio and annealed with the same process of the preparation of Leaf4 structure.

Leaf4 closure experiment design. The original closure strand at the apex of each blade was replaced with a new strand designed such that each strand is complementary to half of the adjacent blade's apex sequence, but collectively span the gap to facilitate closure.

Blade surface target capture (bulge formation) experiment design. Two staple strands located in the middle region of each blade were extended. The sequence of each extension represents half of the sequence complementary to the target sequence.

Two cloverleaf sandwich assembly experiment design. The two middle staple strands on each blade were extended. On one set of blades (belonging to one Lucky4 unit), the extended sequences corresponded to one half of the sequence complementary to the target sequence. On the other set of blades (belonging to the second Lucky4 unit), the extended sequences corresponded to the other half of the sequence complementary to the target sequence. Hybridization with the full target sequence bridges the two units, forming the sandwich structure.

Construction of the cloverleaf DNA origami and its derivatives

The structure design for the origami is presented in Fig. S1, and sequences of the staple strands are listed in Table S1. All the origami strands including target strands were purchased from Sangon Biotech (Shanghai, China), and dissolved in a folding buffer containing 1× Tris-acetate-EDTA (TAE) buffer and 12.5 nM $MgCl_2$ to get a final concentration of 100 μM. For the origami preparation, a one-pot reaction was carried out by first mixing the M13mp18 scaffold with 5 to 15× excess of staple strands in the folding buffer, followed by a thermal annealing process in a Thermal Cycler. Specifically, the annealing process is linearly from 95 °C to 4 °C for 12 h. The derivatives of the origami were also prepared according to this annealing process. As for the target capturing experiments or the strand displacement experiments, the reaction was performed from 45 °C to 35 °C for 6 h.

AFM characterization

All of the samples were characterized using AFM in water tapping mode on a Cypher ES Environmental Atomic Force Microscope (Oxford). 5 μL of fresh samples after annealing were diluted in 1× TAE/Mg^{2+} buffer and pipetted onto the freshly cleaved mica surface. Incubate the sample on the mica surface for 5 minutes for the absorption. Then add another 30 μL of 1× TAE/Mg^{2+} buffer before scanning with AFM.

Results and discussion

Construction of the cloverleaf DNA origami

As illustrated in Fig. 1A, two basic cloverleaf related DNA origami structures were prepared. In the absence of the central

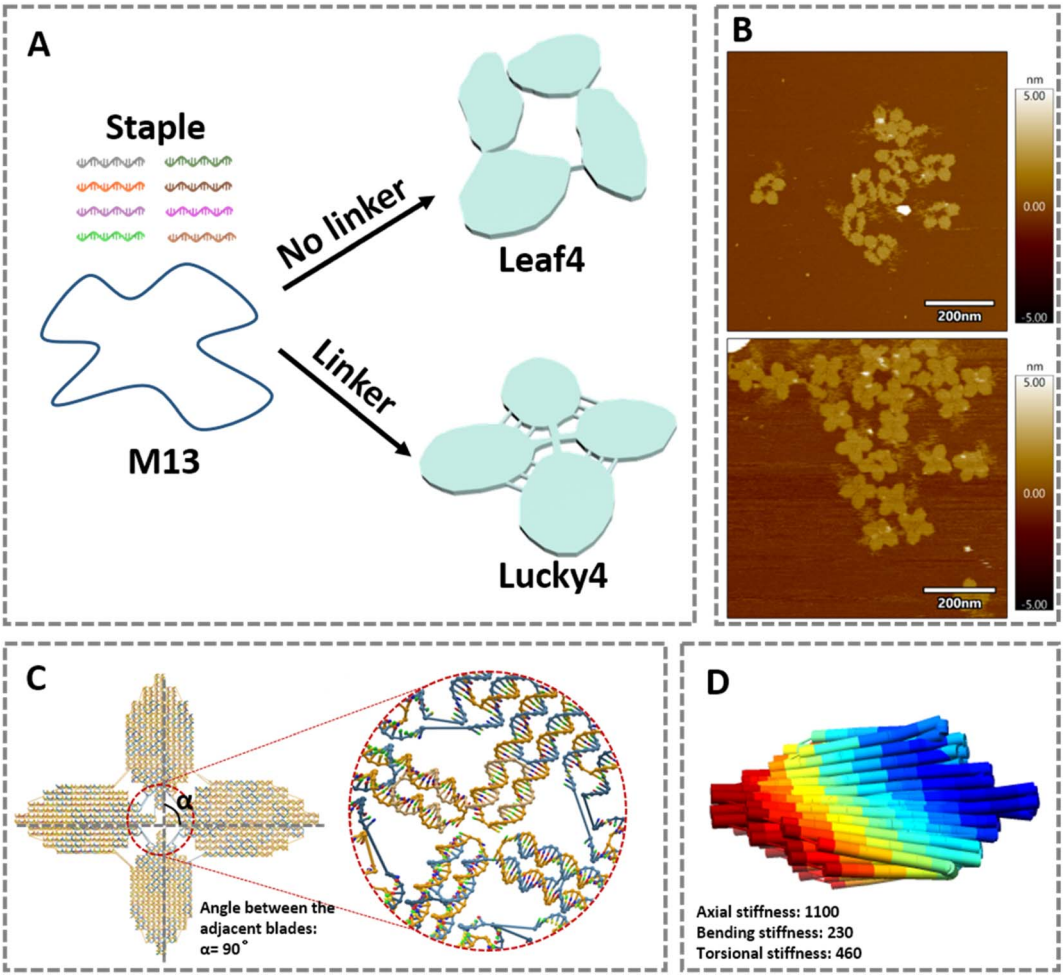

Fig. 1 (A) Schematic illustration of the preparation and morphologies of the Leaf4 and Lucky4 origami structures. Without the addition of the central staple strands (termed linker strands), a loose four-leaf structure (termed Leaf4) forms. Upon addition of the linker strands, a four-leaf clover structure (termed Lucky4) forms. (B) Atomic force microscopy (AFM) characterization of Leaf4 and Lucky4 origami morphologies. Leaf4 leaves predominantly exhibit two distinct structural morphologies, resulting in an overall irregular structure. In contrast, Lucky4 leaves display relatively uniform structures, and the overall structure presents a regular four-leaf clover morphology. (C) TacoxDNA simulation of the Lucky4 origami structure. The insert shows the cross-shaped junction formed between the origami leaves upon incorporation of the linker strands. (D) CanDo simulation depicting the energy-minimized state of the Lucky4 origami. This indicates that the stacked conformation is the most stable state for the origami structure.

staple strands, termed linker strands, a loose four-leaf structure known as Leaf4 was formed. Whereas upon the addition of these linker strands, the structure transformed into a well-defined four-leaf clover morphology, termed Lucky4. AFM was employed to characterize the morphologies of both Leaf4 and Lucky4 origami structures (Fig. 1B). Leaf4 structures predominantly exhibited two distinct structural morphologies, leading to an overall irregular appearance. Conversely, Lucky4 structures displayed relatively uniform leaf morphologies, resulting in a regular four-leaf clover shape. The successful formation of both Leaf4 and Lucky4 origami structures underscores the precision and versatility of DNA origami technology. The transformation from Leaf4 to Lucky4 upon the addition of linker strands highlights the critical role of these strands in determining the overall morphology of the origami structures. The AFM characterizations provided valuable insights into the structural differences between Leaf4 and Lucky4. The irregular appearance of Leaf4 structures, in contrast to the uniform and regular morphology of Lucky4, underscores the importance of linker strands in achieving well-defined origami shapes. The linker strands hybridize with scaffold sequences of adjacent blades, forming a double-helical structure between every two blades and pulling them together. Thus with all linker strands, the four blades were pulled tightly together and rearranged into a cross-shaped structure, thereby enhancing the rigidity of the origami.

Furthermore, tacoxDNA simulations were conducted to visualize the Lucky4 origami structure (Fig. 1C). The insert within this figure highlighted the cross-shaped junctions formed between the origami blades upon the incorporation of linker strands. Additionally, CanDo simulations were performed to determine the energy-minimized state of the Lucky4

origami, suggesting that the stacked conformation was the most stable state for this structure (Fig. 1D). The tacoxDNA and CanDo simulations further supported these findings, providing visual evidence of the cross-shaped junctions formed in Lucky4 and the stability of its stacked conformation.

Dimensional details of both Leaf4 and Lucky4 origami structures were precisely measured and the results were shown in Fig. 2. The blades were approximated as ellipses, with their major and minor axis lengths recorded. And the aspect ratios (major axis/minor axis) of the blades were calculated. In Leaf4, the aspect ratios of the two blades were 2.4 and 1.2, respectively, whereas all blades in Lucky4 had an aspect ratio of 1.2 (Fig. 2C). The overall structure was approximated as a rectangle, with its length and width measured. The overall dimensions of Leaf4 were 120 nm in length and 80 nm in width, whereas those of Lucky4 were approximately 102 nm in both dimensions (Fig. 2D). The assembly yields for Leaf4 and Lucky4 structures were found to be high, at 91% and 90%, respectively (Fig. 2B). The yield was calculated by first counting the successful structures in the field of AFM view and dividing it by the counts of all structures (including malformed ones). To ensure the uniformity of the AFM view, the observed sample was first diluted and evenly pipetted onto a freshly mica surface before scanning. Analysis of the individual blades within both Leaf4 and Lucky4 origami structures revealed similar average area and perimeter values (Fig. 2E and F). The high assembly yields obtained for both Leaf4 and Lucky4 structures demonstrate the efficiency and reliability of the DNA origami assembly process. The aspect ratios and dimensional measurements provided a comprehensive understanding of the structural features of these origami shapes. The similarity in average area and perimeter values of the individual blades within both structures suggests that despite their morphological differences, they share fundamental geometric properties.

Programmable reconfiguration of Leaf4 origami

The inherently flexible Leaf4 origami structure was dynamically reconfigured from an open state to a closed, doughnut-shaped topology (Fig. 3A). This was achieved by replacing original apex staple strands (a and b) with chimeric "strand c" designed to hybridize across adjacent blade apexes (Fig. 3B). AFM confirmed successful closure, with tethered structures exhibiting a characteristic donut morphology and an area distribution

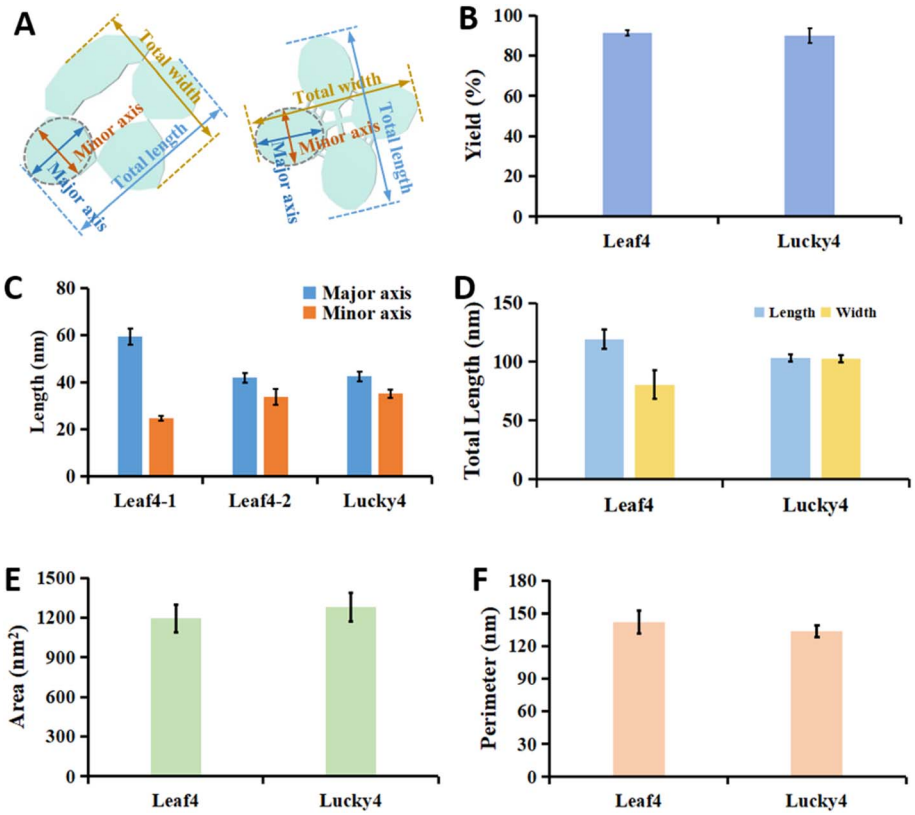

Fig. 2 (A) Schematic illustration showing the specific dimensional details of the Leaf4 and Lucky4 origami structures. The blades are approximated as ellipses, with their major and minor axis lengths measured. The entire structure is approximated as a rectangle, with its overall length and width measured. (B) The assembly yields of the Leaf4 and Lucky4 origami structures are 91% and 90%, respectively. (C) The aspect ratios (length/width) of the two blades in Leaf4 are 2.4 and 1.2, respectively, while both blades in Lucky4 have an aspect ratio of 1.2. (D) The overall length and width of the Leaf4 origami structure are 120 nm and 80 nm, respectively, while those of the Lucky4 origami structure are both approximately 102 nm. The (E) average area and (F) average perimeter values of the individual blades in both Leaf4 and Lucky4 origami structures are similar.

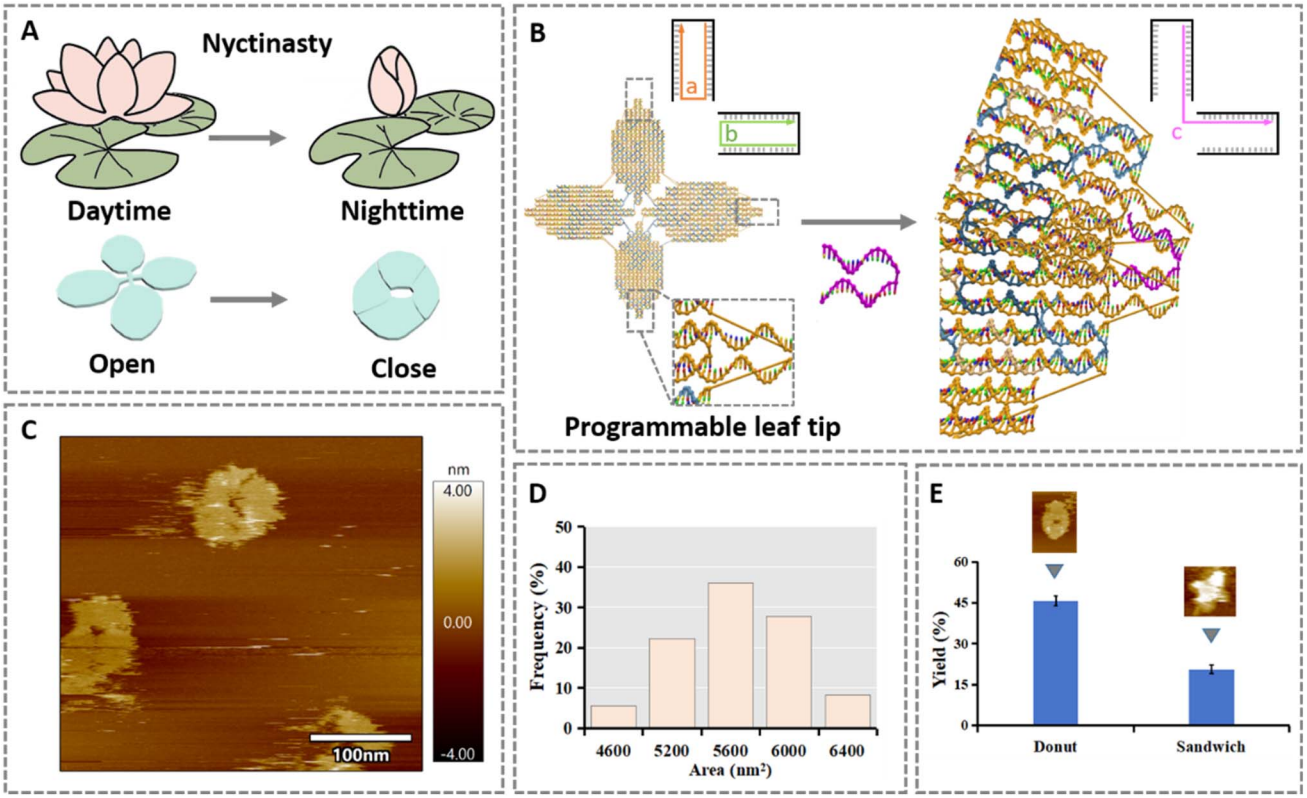

Fig. 3 (A) Schematic illustration of the Leaf4 origami transitioning from an open to a closed state, analogous to the daytime blooming and nocturnal closing of Nymphaea (water lilies) in nature. (B) The apexes of the Leaf4 origami blades can be programmably modified. Staple strands a and b shown in the diagram close the origami scaffold at adjacent blade apexes. By replacing strands a and b with strand c (where the first half of c is identical to a and the second half identical to b), adjacent blades become tethered. This strand replacement process is repeated for all original apex staples, achieving full closure of the origami structure. (C) AFM image showing the structure after replacement of all Leaf4 apex staples. Tethering adjacent blades results in a doughnut-shaped topology. (D) Area distribution of Leaf4 origami structures after apex staple replacement (predominantly 5000–6000 nm^2). (E) Yield of doughnut-shaped structures formed by blade tethering (~45%), and yield of sandwich structures formed by stacking two four-leaf clover origami units in subsequent experiments (~20%).

predominantly between 5000–6000 nm^2 (Fig. 3C and D). The yield of this biomimetic transition, inspired by water lily closure, reached ~45% (Fig. 3E). The controlled closure of Leaf4 demonstrates the potential of DNA origami as a platform for dynamic nanomachines. The Leaf4 transition to a closed state exemplifies nature-mimetic design, akin to plant structures like water lily, which optimize environmental responses through reversible conformational changes. This adaptability could inform responsive material systems for targeted delivery or sensing. While effective, the moderate yield suggests kinetic challenges in simultaneous strand displacement and hybridization at multiple apexes.

Reversible target capture and release on Lucky4 blades

The blades of the stable Lucky4 clover were functionalized with split capture sequences displayed on extended staple strands (Fig. 4A). Upon adding a toehold-bearing target sequence, hybridization formed double-stranded regions on the blades, increasing local height by ~1 nm (from ~2 nm to ~3 nm) as measured by AFM (Fig. 4B and C). Subsequent addition of a toehold-complementary displacement strand efficiently released the target, resetting the blades to their original height (~2 nm) (Fig. 4B and D), demonstrating reversible molecular capture. After adding the target strand, the capture strand hybridizes with the target strand, forming a double-helical structure. For the capture strand retains 5 nt unpaired bases forming a short single-stranded overhang (the teohold) after capturing the target molecule. When a releasing strand that is fully complementary to the capture strand is added, it hybridizes with the capture strand *via* the toehold domain, triggering branch migration and ultimately forming a longer double-stranded structure, thereby releasing the shorter target molecule. The essence of strand displacement reactions is the structural reorganization of DNA molecules through dynamic equilibrium. The temperature 45 °C to 35 °C can accelerate the rate of the strand displacement without compromising origami integrity, as demonstrated in entropy-driven systems.[24] Lucky4's spatially addressable blades provide an ideal scaffold for reversible molecular interactions. The observed 1 nm height increase upon target capture is consistent with the formation of rigid double-stranded DNA (dsDNA) on the origami surface. Crucially, the incorporation of a toehold domain enables

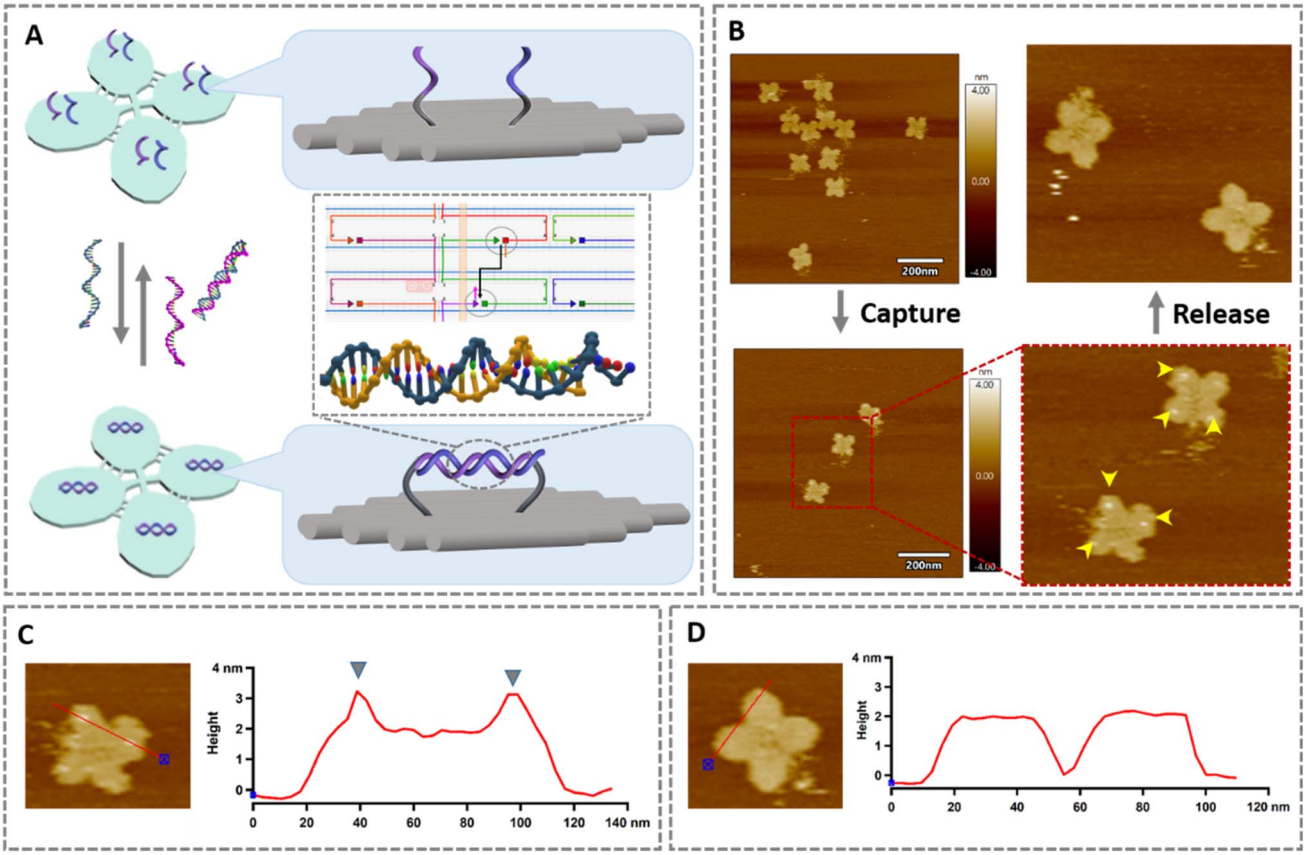

Fig. 4 (A) Schematic illustration showing the functionalization process on each blade of the four-leaf clover origami. Two staple strands are extended to display half of a DNA single strand complementary to the target sequence, respectively. Upon addition of the target sequence bearing a toehold domain, double-stranded structures form on the blade surfaces. Subsequent addition of a DNA strand complementary to the toehold-bearing strand displaces the target sequence, releasing the origami and surface modifications. The insert shows a schematic of the double-stranded structure formed by the modification strand bound to the target sequence (tacoxDNA), and the positioning of the modification sites within the caDNAno design. (B) AFM images characterizing the four-leaf clover origami structure: (i) before target sequence capture, (ii) after target sequence capture, and (iii) after target sequence release. (C) Height distribution profile of the four-leaf clover origami after target sequence capture. The height at the target binding locations increases by approximately 1 nm. (D) Height distribution profile of the four-leaf clover structure after target sequence release. The blades exhibit a relatively uniform height of approximately 2 nm.

efficient strand displacement, allowing for cyclical capture and release – a critical feature for reusable biosensors or responsive materials. Functionalization and reversible target capture/release demonstrate precision in strand displacement mechanisms, allowing controlled surface modifications. The ~1 nm height increase upon binding provides a quantifiable metric for detecting molecular interactions, potentially enhancing biosensing platforms that leverage toehold-mediated dynamics.

Compared to simpler origami geometries such as triangular or cross-shaped structures, the cloverleaf shape has the advantage of both flexibility and rigidity. The flexibility enables the biomimetic reconfiguration of the origami, simulating water lily closure, whereas the rigidity makes the origami a suitable substrate for incorporating capture strands and capturing target molecules.

Higher-order assembly into sandwich structures

Two distinct Lucky4 origami units were functionalized with split capture sequences on their blades. Adding the target sequence bridged complementary strands across units, inducing face-to-face stacking into "sandwich" structures (Fig. 5A). AFM confirmed successful dimerization, with sandwich structures exhibiting a height (~4 nm) approximately double that of single units (~2 nm) (Fig. 5B and C). 3D height maps visually distinguished the dimers from monomers (Fig. 5D). The assembly yield reached ~20% (Fig. 3E). The yield was calculated by multiplying the number of sandwich structures by 2 and then dividing by the total number of all origami structures. The successful assembly of sandwich structures highlights the potential for programmable higher-order architectures. The doubling in height provides unambiguous confirmation of face-to-face stacking. While the yield is lower than the monomeric functionalization, it establishes a proof-of-concept for using target-specific hybridization to drive the assembly of complex, multi-origami nanostructures. Factors influencing yield likely include steric constraints during dimerization and potential non-specific aggregation.

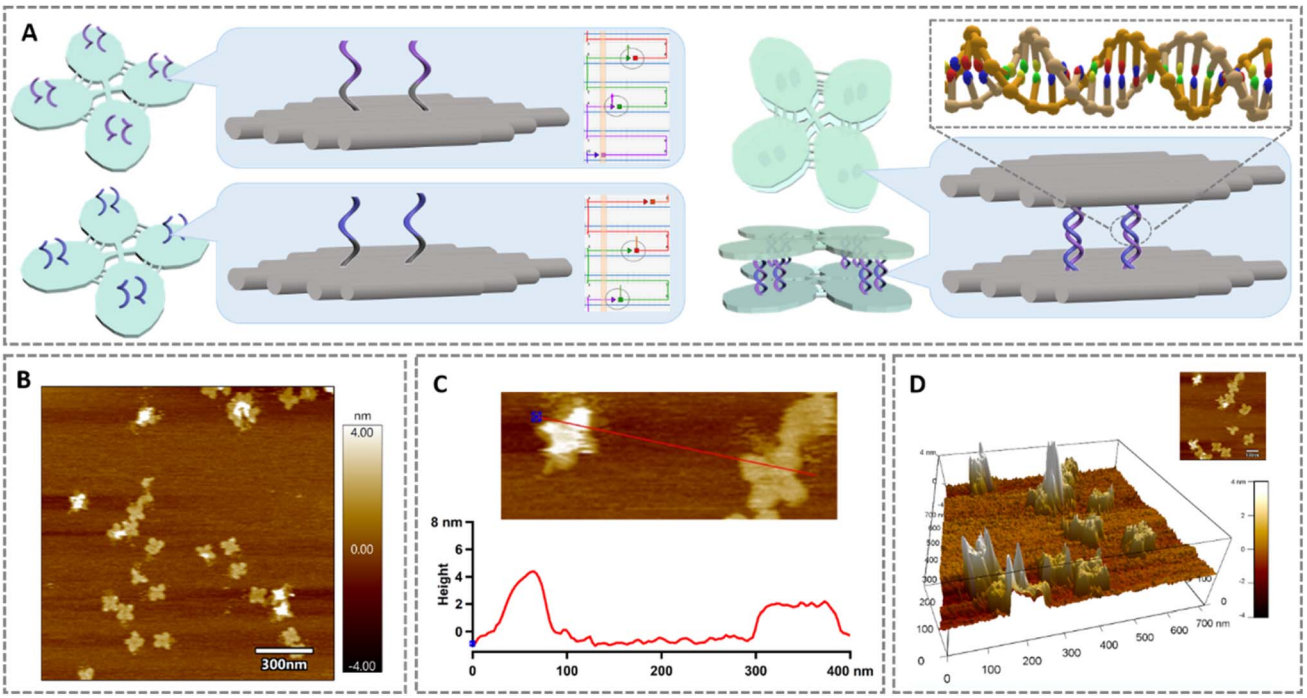

Fig. 5 (A) Schematic illustrating the functionalization strategy for two sets of four-leaf clover origami units. Each blade is modified with staple strand extensions displaying half of a DNA sequence complementary to the target sequence. Upon addition of the target sequence, it hybridizes with the complementary half-sequences on blades from both origami units, tethering the two four-leaf clover origamis together and inducing their stacking into a sandwich structure. (B) AFM characterization of origami structures after target sequence addition, showing individual four-leaf clover units alongside tethered pairs forming sandwich structures. (C) Comparative height distribution profiles of sandwich structures *versus* single four-leaf clover units. Sandwich structures exhibit a height approximately double that of single units (4 nm *vs.* 2 nm). (D) Three-dimensional AFM height map of a representative field of view after target sequence addition, demonstrating the distinct height difference between individual four-leaf clover structures (lower) and sandwich structures (higher).

Conclusion

This study demonstrates the cloverleaf DNA origami system as a multifunctional platform integrating structural reconfiguration (Leaf4's water lily-inspired closure), dynamic molecular sensing (Lucky4's reversible capture/release *via* toehold-mediated strand displacement), and programmable higher-order assembly (target-triggered sandwich structures). The system's versatility stems from three key design principles: (i) architectural control through strategic staple placement (central linkers in Lucky4 *vs.* flexible apex strands in Leaf4), (ii) split capture strand functionalization enabling both visual detection (~1 nm AFM height change) and supramolecular recognition, and (iii) modular toehold sequences permitting spatiotemporal control over all transitions. By bridging biomimetic structural dynamics with molecular programmability, this work establishes a paradigm for developing responsive nanodevices in biosensing, drug delivery, and adaptive nanomaterials.

Conflicts of interest

There are no conflicts of interest to declare.

Data availability

The datasets used and/or analysed during the current study available from the corresponding author on reasonable request.

Supplementary information is available. See DOI: **https://doi.org/10.1039/d5ra06047h**.

Acknowledgements

This work is supported by the National Natural Science Foundation of China with grant No. 62202112, 62072129, 62172114 and 6172376, the State Key Program of National Natural Science of China with grant No. 62332006, the National Key R&D Program of China with grant No. 2019YFA0706401.

References

1 H. Lv, N. Xie, M. Li, M. Dong, C. Sun, Q. Zhang, L. Zhao, J. Li, X. Zuo, H. Chen, *et al.*, DNA-based programmable gate arrays for general-purpose DNA computing, *Nature*, 2023, **622**(7982), 292.

2 S. Dey, C. Fan, K. V. Gothelf, J. Li, C. Lin, L. Liu, N. Liu, M. A. D. Nijenhuis, B. Saccà, F. C. Simmel, *et al.*, DNA origami, *Nat. Rev. Methods Primers*, 2021, **1**(1), 13.

3 F. Hong, F. Zhang, Y. Liu and H. Yan, DNA Origami: Scaffolds for Creating Higher Order Structures, *Chem. Rev.*, 2017, **117**(20), 12584.

4 J. Xu, W. Liu, K. Zhang and E. Zhu, Dna coding theory and algorithms, *Artif. Intell. Rev.*, 2025, **58**(6), 178.

5 M. Glaser, S. Deb, F. Seier, A. Agrawal, T. Liedl, S. Douglas, M. K. Gupta and D. M. Smith, The Art of Designing DNA Nanostructures with CAD Software, *Molecules*, 2021, **26**(8), 2287.

6 S. Nummelin, J. Kommeri, M. A. Kostiainen and V. Linko, Evolution of Structural DNA Nanotechnology, *Adv. Mater.*, 2018, **30**(24), 1703721.

7 P. Piskunen, S. A.-O. Nummelin, B. Shen, M. A.-O. Kostiainen and V. A.-O. Linko, Increasing Complexity in Wireframe DNA Nanostructures, *Molecules*, 2020, **25**(8), 1823.

8 W. Liu, H. Zhong, R. Fau - Wang, N. C. Wang R Fau - Seeman and N. C. Seeman, *Crystalline Two-Dimensional DNA-Origami Arrays*, pp. , pp. 1521–3773.

9 C. Chen, T. Lin, M. Ma, X. Shi and X. Li, Programmable and scalable assembly of a flexible hexagonal DNA origami, *Nanotechnology*, 2021, **33**(10), 105606.

10 C. Chen, J. Xu, L. Ruan, H. Zhao, X. Li and X. Shi, DNA origami frame filled with two types of single-stranded tiles, *Nanoscale*, 2022, **14**(14), 5340.

11 G. Tikhomirov, P. Petersen and L. Qian, Fractal assembly of micrometre-scale DNA origami arrays with arbitrary patterns, *Nature*, 2017, **552**(7683), 67.

12 P. Petersen, G. Tikhomirov and L. Qian, Information-based autonomous reconfiguration in systems of interacting DNA nanostructures, *Nat. Commun.*, 2018, **9**(1), 5362.

13 N. Sarraf, K. R. Rodriguez and L. Qian, Modular reconfiguration of DNA origami assemblies using tile displacement, *Sci. Robot.*, 2023, **8**(77), eadf1511.

14 S. Julin, V. Linko and M. A. Kostiainen, Reconfigurable pH-Responsive DNA Origami Lattices, *ACS Nano*, 2023, **17**(11), 11014.

15 M. Kim, C. Lee, K. Jeon, J. Y. Lee, Y.-J. Kim, J. G. Lee, H. Kim, M. Cho and D.-N. Kim, Harnessing a paper-folding mechanism for reconfigurable DNA origami, *Nature*, 2023, **619**(7968), 78.

16 G. Tikhomirov, P. Petersen and L. Qian, Triangular DNA Origami Tilings, *J. Am. Chem. Soc.*, 2018, **140**(50), 17361.

17 P. W. K. Rothemund, Folding DNA to create nanoscale shapes and patterns, *Nature*, 2006, **440**(7082), 297.

18 F. Wang, X. Shi, X. Chen, D. Deng, S. Li, S. Sun, Z. Kou, J. Xu and X. Qiang, Instruction-responsive programmable assemblies with DNA origami block pieces, *Nucleic Acids Res.*, 2024, **53**(1), gkae1193.

19 D. Wang, Y. Fu, J. Yan, B. Zhao, B. Dai, J. Chao, H. Liu, D. He, Y. Zhang, C. Fan, *et al.*, Molecular Logic Gates on DNA Origami Nanostructures for MicroRNA Diagnostics, *Anal. Chem.*, 2014, **86**(4), 1932.

20 D. Selnihhin, S. M. Sparvath, S. Preus, V. Birkedal and E. S. Andersen, Multifluorophore DNA Origami Beacon as a Biosensing Platform, *ACS Nano*, 2018, **12**(6), 5699.

21 J. Dai, C. Xing, Y. Lin, Y. Huang, Y. Yang, Z. Chen, C. Lu and H. Yang, Localized DNA catalytic hairpin assembly reaction on DNA origami for tumor-associated microRNA detection and imaging in live cells, *Sens. Actuators, B*, 2021, **344**, 130195.

22 C. Xing, S. Chen, Q. Lin, Y. Lin, M. Wang, J. Wang and C. Lu, An aptamer-tethered DNA origami amplifier for sensitive and accurate imaging of intracellular microRNA, *Nanoscale*, 2022, **14**(4), 1327.

23 S. Sun, J.-D. Wen, Q.-R. Xiao, X.-L. Qiang and X.-L. Shi, Molecular logic gates based on programmable self-assembly of DNA origami triangles for the detection of nucleic acid molecules, *Sci. Rep.*, 2025, **15**(1), 29178.

24 C. Chen, J. Xu and X. Shi, Adjusting Linking Strands to Form Size-Controllable DNA Origami Rings, *IEEE Trans. Nanobiosci.*, 2020, **19**(2), 167.